Flow Film Boiling from a Sphere and a Horizontal Cylinder Embedded in Porous Medium

J. Orozco,* D. Poulikakos,† and M. Gutjahr‡
University of Illinois at Chicago, Chicago, Illinois

This paper focuses on the problem of flow film boiling from a body embedded in a porous medium. Two body geometries are investigated thoroughly: a horizontal cylinder and a sphere. The theoretical model relies on the Brinkman-extended flow model to describe the flow inside the thin vapor layer occupying the neighborhood near the heated surface. Unlike the counterpart of the present problem in classical fluids, it was found that the flow reversal does not occur inside the vapor layer. The effects of subcooling, incoming liquid flow velocity, and Darcy number on the heat and fluid flow characteristics of the problem are thoroughly documented. Finally, the overall and local heat-transfer rates from the surface to the fluid are determined for a wide range of the problem parameters and reported with the help of the conduction referenced Nusselt number.

Nomenclature

A = dimensionless group, Eq. (17)
B = dimensionless group, Eq. (18)
$\cosh(x)$ = hyperbolic cosine of x
$\coth(x)$ = hyperbolic cotangent of x
$\operatorname{csch}(x)$ = hyperbolic cosecant of x
D = diameter of sphere or cylinder
Da = modified Darcy number, Eq. (9)
h = local heat-transfer coefficient
h_{fg} = latent heat of vaporization including the effects of vapor superheat
K = permeability
k_l = effective thermal conductivity of porous medium in the liquid region
k_v = effective thermal conductivity of porous medium in the vapor film
L = cylinder length
M = dimensionless group, Eq. (21)
m = vapor mass flow rate
N = dimensionless group, Eq. (22)
Nu = local Nusselt number, Eq. (25)
$\overline{Nu}$ = overall Nusselt number, $(1/S)\int_S Nu\, dS$
P = pressure
q = Heat flux
R = radius of sphere or cylinder
S = surface area
$\sinh(x)$ = hyperbolic sine of x
T = temperature
ΔT_l = temperature difference, $T_{sat} - T_B$
ΔT_v = temperature difference, $T_w - T_{sat}$
u = x velocity component
$\bar{u}$ = average velocity, $(1/\delta)\int_0^\delta u\, dy$
U_∞ = bulk liquid velocity
v = y velocity component
x = curvilinear coordinate, Fig. 1
y = curvilinear coordinate, Fig. 1
α = thermal diffusivity
δ = vapor film thickness
θ = angle measured from forward stagnation point, Fig. 1
μ = fluid viscosity
$\tilde{\mu}$ = effective fluid viscosity in porous medium
ρ = density

Subscripts

B = bulk
l = liquid region
sat = saturation
v = vapor region
w = wall
$*$ = dimensionless quantity

Received Feb. 6, 1987; revision received Sept. 2, 1987.

*Assistant Professor, Department of Mechanical Engineering.
†Associate Professor, Department of Mechanical Engineering.
‡Graduate Research Assistant, Department of Mechanical Engineering.

Introduction

BOILING heat transfer in porous media has a wide range of important engineering applications, from geothermal systems and oil recovery to the chemical and nuclear industries. Undoubtedly, the theoretical treatment of two-phase flow and heat transfer in porous media is complex. As discussed by Cheng,[1] to model two-phase flow in porous media while using the popular Darcy model, one needs to introduce the concept of relative permeability to account for the fact that some of the pore spaces are filled partly with vapor and partly with liquid. However, because of the mathematical complexity of the equations involving the relative permeability, analytical solutions for two-phase flow problems (such as boiling) in porous media can be obtained only with the help of simplifying assumptions. Perhaps the most important modeling assumption is that the two phases (liquid and vapor) are separated by a *distinct* boundary without a two-phase zone between them.[1,2] This assumption circumvents the mathematical complexities that the use of the relative permeability introduces.

Unlike the two-phase flow in classical fluids (which constitutes a distinct subfield in heat-transfer research), two-phase flow in porous media has received considerably less attention. With reference to film boiling in particular, Cheng and Verma[2] first theoretically studied the problem of boiling from a flat plate in a porous medium. Also theoretical is the work of Ip and Minkowycz,[3] which focused on the phenomenon of film boiling about a vertical cylinder embedded in a porous medium in the presence of an axial pressure gradient.

Experimental studies of boiling in porous media have also been reported in the literature. For example, Chuah and Carey[4] presented experimental data pertaining to the effect of a thin layer of unconfined particles on saturated pool boiling heat transfer from a horizontal surface. Tsung et al.[5] carried out an experimental study of boiling heat transfer from a sphere embedded in porous media composed of nonheated

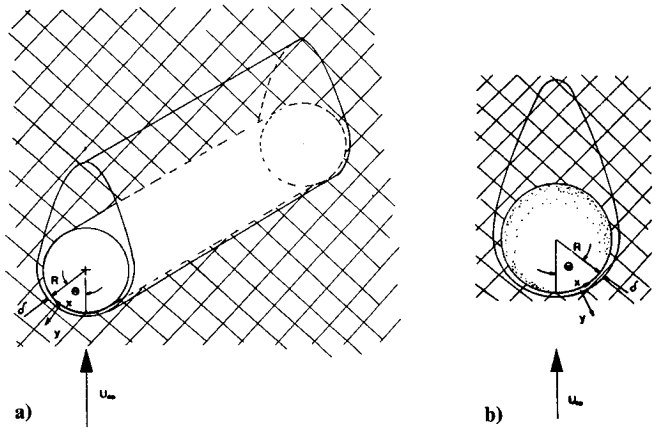

Fig. 1 Two geometries of interest: a) a horizontal cylinder placed in a porous medium, and b) a sphere placed in porous medium.

glass particles under steady-state and transient quenching conditions.

Clearly, more studies are needed to improve our fundamental knowledge of boiling heat transfer in porous media. The present paper presents such a study. In particular, the problem of flow film boiling from both a sphere and a cylinder is modeled theoretically. Since the vapor film occupies a thin region near the cylinder or the sphere surface, the Brinkman-modified Darcy model is used to describe the flow inside the vapor film. This model has proved especially appropriate for flows near solid boundaries.[6–8] Outside the vapor film, potential flow is assumed. This assumption is appropriate if the Darcy flow model is applicable in the region outside the vapor film. The results reported in this paper document the dependence of the temperature and flowfield inside the vapor film on the problem parameters for both the basic geometries under investigation, namely, the cylinder and sphere.

Theoretical Model

The two geometrical configurations of interest in this study are shown schematically in Fig. 1. Figure 1a pertains to the horizontal cylinder and Fig. 1b to the sphere. In both cases, it is assumed that the flow boiling phenomenon is of the filmwise type and that the vapor film thickness is small compared to the body diameter. The mathematical modeling of the problem follows the main principles and it is subject to the same approximations with those reported in Ref. 9. In this reference, Witte and Orozco studied theoretically flow film boiling from bodies submerged in a Newtonian fluid. For the sake of brevity, details of the procedures and approximations in Ref. 9 will not be included here.

The mathematical models for the cylinder and sphere are conceptually identical. Therefore, only the model for the cylinder will be presented in detail here. Selected key results for the spherical geometry will also be outlined. It is assumed that the vapor layer occupies a thin region near the surface of the cylinder. As discussed in the introduction, it has been found that the Brinkman-modified Darcy model is appropriate for flows near solid boundaries in porous media. Hence, we chose to adopt this model for the flow inside the vapor film. Outside the vapor film (in the liquid region), we assumed potential flow.[9] The potential flow assumption requires that the Darcy flow model be valid in the liquid region.[10] Since the liquid region is separated from the solid cylinder surface by the vapor region, it is felt that the Darcy model is appropriate to describe the flowfield inside the liquid region. After the usual boundary-layer assumptions are taken into account, the Brinkman-Darcy momentum equation for the vapor region reads

$$\frac{dp}{dx} = -\frac{\mu_v u_v}{K} + \tilde{\mu}_v \frac{d^2 u_v}{dy^2} \tag{1}$$

where x and y are the curvilinear coordinates (Fig. 1), p the pressure, u_v the vapor velocity component in the x direction, K the permeability, μ the vapor viscosity, and $\tilde{\mu}_v$ the effective vapor viscosity in the porous medium.

The velocity field in the vapor region satisfies the following boundary conditions

$$u_v = 0 \text{ at } y = 0 \tag{2}$$

$$u_v = u_l \text{ at } y = \delta \tag{3}$$

where δ is the thickness of the vapor layer.

It is well known that a flow potential can be defined for flow in Darcy porous media because of the form of the Darcy momentum equation. Therefore, velocity distributions around bodies in Darcy porous media can be described mathematically by using the principles of potential flow theory. This does not mean that the flow in the porous matrix is inviscid. On the contrary, the Darcy momentum equation still represents a balance between the pressure gradient and the Darcy friction. However, the mathematical analysis leading to the flowfield is simplified considerably by introducing a flow potential that works much in like potential flows in classical fluids. On the other hand, unlike classical fluids, the pressure field is related to the velocity field with the help of the Darcy momentum equation—not with Bernoulli's equation. Because of this fact, the results for a classical fluid in Ref. 9 cannot be reproduced in the present work even if the Darcy term in Eq. (1) is neglected. For more details on the existence of a flow potential in the Darcy flow in porous media, Ref. 10 is recommended. Based on this discussion, the liquid velocity at the liquid/vapor interface is

$$u_l = 2\, U_\infty \sin\theta \tag{4}$$

Following Refs. 11 and 12, we next assume that the liquid pressure is imposed upon the vapor layer; this assumption yields

$$\left(\frac{dp}{dx}\right)_v = \left(\frac{dp}{dx}\right)_l \tag{5}$$

The pressure gradient in the liquid region is easily calculated from the Darcy momentum equation for the liquid region

$$\left(\frac{dp}{dx}\right)_l = -\frac{\mu_l}{K} u_l \tag{6}$$

where μ_l is the liquid viscosity.

It is worth clarifying that the radial component of liquid velocity (and the related pressure drop) is neglected in the present analysis. This component of velocity is given by

$$v_l = -U_\infty [1 - R^2/(R+x)^2] \sin\theta$$

at the liquid/vapor interface $x \sim \delta$. Since $\delta \ll R$, it is clear from the above that $v_l \approx 0$. The same was adopted successfully in Ref. 9.

Equations (1–6) contain enough information to allow for the calculation of the velocity field inside the vapor layer. More specifically, the pressure gradient in Eq. (1) is calculated via Eqs. (4–6). Next, Eq. (1) is integrated analytically subject to Eqs. (2) and (3) to yield

$$u_v = 2U_\infty \sin\theta \frac{\sinh(Da^{-\frac{1}{2}} y_*)}{\sinh(Da^{-\frac{1}{2}} \delta_*)} + \frac{\mu_l}{\mu_v}(2U_\infty \sin\theta) \times \left\{1 + \frac{\sinh[Da^{-\frac{1}{2}}(y_* - \delta_*)] - \sinh(Da^{-\frac{1}{2}} y_*)}{\sinh(Da^{-\frac{1}{2}} \delta_*)}\right\} \tag{7}$$

In the above equation, subscript * denotes the dimensionless quantities and Da is the Darcy number

$$(y_*, \delta_*) = \frac{(y,\delta)}{D} \tag{8}$$

$$Da = \frac{K}{D^2}\frac{\tilde{\mu}_v}{\mu_v} \tag{9}$$

The procedure for the calculation of the vapor velocity field for the spherical geometry is identical to the procedure outlined above, with the difference that the velocity of the liquid region for the sphere (potential flow) is

$$u_l = \frac{3}{2} U_\infty \sin\theta \tag{10}$$

The final result for the velocity field is the vapor film surrounding the sphere is

$$u_v = \frac{3}{2} U_\infty \sin\theta \frac{\sinh(Da^{-\frac{1}{2}} y_*)}{\sinh(Da^{-\frac{1}{2}}\delta_*)} + \frac{\mu_1}{\mu_v}\left(\frac{3}{2} U_\infty \sin\theta\right) \times\left\{1 + \frac{\sinh[Da^{-\frac{1}{2}}(y_* - \delta_*)] - \sinh(Da^{-\frac{1}{2}} y_*)}{\sinh(Da^{-\frac{1}{2}}\delta_*)}\right\} \tag{11}$$

Next, attention is shifted to the temperature field in the vapor film for the cylindrical body. The analysis starts with a mass-energy balance on a differential film element shown in Fig. 2,

$$dq = dq_v + dq_l \tag{12}$$

where dq_v is the energy required to form the vapor and dq_l the energy conducted into the subcooled liquid. Equation (12) can be written as

$$k_v \frac{\Delta T_v}{\delta} R\, d\theta L = h'_{fg}\, d\dot{m} + \left[-k_l\, dS\left(\frac{\partial T_l}{\partial y}\right)_{y=\delta}\right] \tag{13}$$

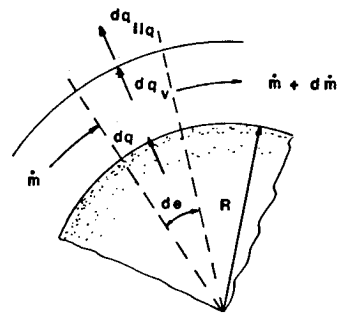

Fig. 2 Differential film element for the energy balance.

where $dS = R\, d\theta L$ and $d\dot{m} = d(\rho_v \bar{u}_v \delta)$. All of the new symbols are defined in the nomenclature. To proceed with the analysis, information is needed for the temperature gradient in the last term on the right side of Eq. (13). Following Refs. 9 and 13, we obtain

$$\left(\frac{dT_l}{dy}\right)_{y=\delta} = -\frac{\Delta T_l(\sin\theta)}{(\pi R\alpha/2U_\infty)^{\frac{1}{2}}(1-\cos\theta)^{\frac{1}{2}}} \tag{14}$$

The derivation of Eq. (14) is based on the existence of potential flow in the liquid region and on the concept that the heat transfer to the liquid takes place within a small region near the liquid/vapor interface. The potential flow assumption is justified in our theory because the Darcy flow model is used for the liquid region. The average velocity for the vapor layer is calculated to be

$$\bar{u}_v = U_\infty \frac{2\sin\theta}{\delta_* Da^{-\frac{1}{2}}\sinh[Da^{-\frac{1}{2}}\delta_*]} \times\left\{\left(1 - 2\frac{\mu_l}{\mu_v}\right)[\cosh(Da^{-\frac{1}{2}}\delta_*) - 1] + \frac{\mu_l}{\mu_v} Da^{-\frac{1}{2}}\delta_* \sinh(Da^{-\frac{1}{2}}\delta_*)\right\} \tag{15}$$

Equations (13–15) can be combined to yield a differential equation for $\delta_*(\theta)$ for the horizontal cylinder,

$$\frac{d\delta_*}{d\theta} = \frac{\left[\frac{A}{\delta_*} - \frac{B\sin\theta}{(1-\cos\theta)^{\frac{1}{2}}}\right]\frac{Da^{-\frac{1}{2}}}{(1-\mu_l/\mu_v)} - \left\{\cos\theta\left[\coth(Da^{-\frac{1}{2}}\delta_*) - \operatorname{csch}(Da^{-\frac{1}{2}}\delta_*) + \frac{\mu_l/\mu_v}{1-2\mu_l/\mu_v} Da^{-\frac{1}{2}}\delta_*\right]\right\}}{Da^{-\frac{1}{2}}\sin\theta\left[\operatorname{csch}^2(Da^{-\frac{1}{2}}\delta_*) + \operatorname{csch}(Da^{-\frac{1}{2}}\delta_*)\coth(Da^{-\frac{1}{2}}\delta_*) + \frac{\mu_l/\mu_v}{1-2\mu_l/\mu_v}\right]} \tag{16}$$

where

$$A = \frac{k_v \Delta T_v}{4\rho_v h'_{fg} D U_\infty} \tag{17}$$

$$B = \frac{k_l \Delta T_l}{2\rho_v h'_{fg}(\pi D\alpha_l U_\infty)^{\frac{1}{2}}} \tag{18}$$

The energy analysis for the sphere is identical. For the sake of completeness, we report only two key results: the temperature gradient on the liquid side analogous to Eq. (14) and the final differential equation for $\delta(\theta)$,

$$\left(\frac{\partial T_l}{\partial y}\right)_{y=\delta} = \frac{-\Delta T_l \sin^2\theta}{\left[\frac{2}{3}\pi\frac{R\alpha_l}{U_\infty}\left(\frac{2}{3} - \cos\theta + \frac{1}{3}\cos^3\theta\right)\right]^{\frac{1}{2}}} \tag{19}$$

$$\frac{d\delta_*}{d\theta} = \frac{\left[\frac{M}{\delta_*} - \frac{N\sin^2\theta}{\left(\frac{2}{3} - \cos\theta - \frac{1}{3}\cos^3\theta\right)^{\frac{1}{2}}}\right]\frac{Da^{-\frac{1}{2}}}{1-2\mu_l/\mu_v} - \left\{2\cos\theta\left[\coth(Da^{-\frac{1}{2}}\delta_*) - \operatorname{csch}(Da^{-\frac{1}{2}}\delta_*) + \frac{\mu_l/\mu_v}{1-2\mu_l/\mu_v} Da^{-\frac{1}{2}}\delta_*\right]\right\}}{Da^{-\frac{1}{2}}\sin\theta\left\{\operatorname{csch}(Da^{-\frac{1}{2}}\delta_*)\left[\coth(Da^{-\frac{1}{2}}\delta_*) - \operatorname{csch}(Da^{-\frac{1}{2}}\delta_*)\right] + \frac{\mu_l/\mu_v}{1-2\mu_l/\mu_v}\right\}} \tag{20}$$

where

$$M = \frac{k_v \Delta T_v}{3DU_\infty \rho_v h'_{fg}} \tag{21}$$

$$N = \frac{k_l \Delta T_l}{(3\pi DU_\infty \alpha_l)^{\frac{1}{2}}\rho_v h'_{fg}} \tag{22}$$

Equations (16) and (20) for the cylinder and for the sphere, respectively, need to be solved numerically to yield the thickness of the vapor film. The numerical integration was performed with the help of the fourth-order Runge-Kutta method.[14] Two major points related to the numerical integration are worth clarifying. First, initial conditions (at $\theta = 0$) are required to start the numerical integration. However, the vapor thickness at $\theta = 0$ is unknown and needs to be calculated. To obtain the vapor thickness at $\theta = 0$, we made use of symmetry and set the left side of Eqs. (16) and (20) equal to zero. Next, we took the limit of the resulting equations for θ approaching zero. In both cases (cylinder and sphere), the above procedure resulted in nonlinear algebraic equations. These equations were

solved numerically each time to yield the value of the vapor thickness at $\theta = 0$. This value made it possible to start the numerical integration of Eqs. (16) and (20). The second point that needs clarification pertains to the fact that our model ceases to be valid if flow reversal takes place. To investigate this point, we calculated the velocity gradients at the wall from Eqs. (7) and (11). Unlike in classical fluid, where a critical angle θ_{crit} exists at which the velocity gradient at the wall diminishes indicating flow reversal for values of the angle θ larger than θ_{crit}[9] we found that in the present porous medium study the velocity gradient remains positive for all values of θ ($0 < \theta < \pi$). See Fig. 1. Therefore, our flow model remains valid at all points around the circumference of the cylinder or the sphere and it is physically correct to perform the numerical integration starting from $\theta = 0$ and ending at $\theta = \pi$. The step for the numerical integration ($\Delta\theta$) was "small enough" so that decreasing the step further had no effect on the results. Typically, about 5000 steps were required to yield accurate results for the sphere and for the cylinder cases.

Once the vapor film is known as a function of the angular position, the velocity field can be calculated from Eqs. (7) and (11). In addition, important heat-transfer results can be obtained pertaining to both the local and the overall heat transfer from the body (sphere or cylinder) to the fluid.

The local heat transfer is given by

$$q'' = k_v \frac{(T_w - T_{sat})}{\delta} \tag{23}$$

since the temperature profile inside the vapor layer is linear. Based on the above equation, it is easy to show that the local heat-transfer coefficient and the local Nusselt number are

$$h = \frac{k_v}{\delta} \tag{24}$$

$$Nu = \frac{hD}{k_v} = \frac{D}{\delta} \tag{25}$$

The overall Nusselt number is obtained in the usual manner by averaging the local Nusselt number over the surface of the body. Since the equations for the velocity fielf showed that no flow reversal will take place, we will integrate over the entire surface of the cylinder or the sphere. The expressions for the overall Nusselt number, therefore, are

$$\overline{Nu} = \frac{1}{\pi}\int_0^{\pi} Nu(\theta)\, d\theta \quad \text{(cylinder)}$$

$$= \frac{1}{2}\int_0^{\pi} Nu(\theta)\sin\theta\, d\theta \quad \text{(sphere)} \tag{26}$$

The integration of Eq. (26) was performed numerically after the value of Nu was obtained.

Results and Discussions

The first results aim to document the effect of subcooling, liquid velocity, and Darcy number on the thickness of the vapor layer. These results are reported in Figs. 3–5. The thickness of the vapor layer is an important quantity for it is related directly to the local and overall heat transfer from the body to the surroundings [Eqs. (23–26)]. The effect of subcooling is shown in Fig. 3. Increasing the degree of subcooling from 0 to 30 deg and then to 50 deg yields thinner vapor film thicknesses for both the sphere and the cylinder. Both the thickness, as well as the rate of increase of thickness of the vapor film, increase as the angle θ increases. For a prescribed subcooling, in all cases, the vapor film for the cylinder is thicker than the vapor film for the sphere for small values of θ. As θ increases, after a specific value of θ, the sphere film thickness exceeds the cylinder film thickness and remains the larger of the two thicknesses thereafter.

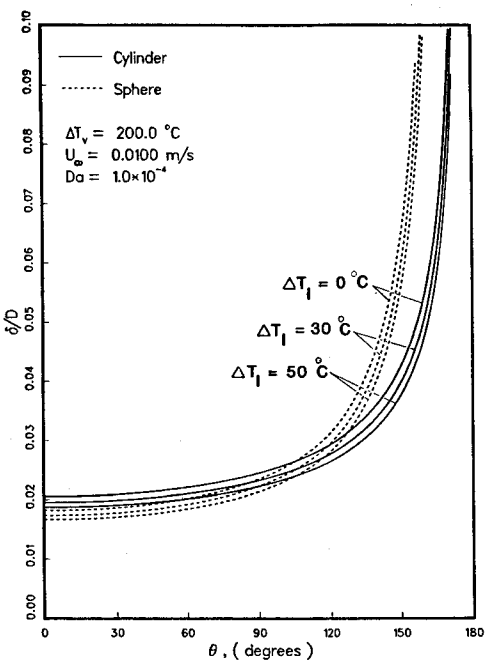

Fig. 3 The effect of subcooling on the vapor film thickness: $Da = 10^{-4}$, $U_\infty = 0.01$ m/s ($A = 1.32 \times 10^{-2}$, $M = 1.80 \times 10^{-2}$).

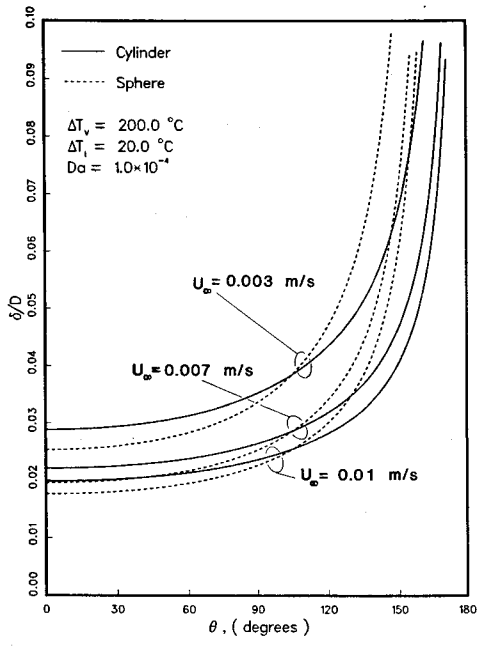

Fig. 4 The effect of liquid velocity on the vapor film thickness: $Da = 10^{-4}$, $\Delta T_l = 20°C$.

Examining Fig. 4 indicates that the effect of the liquid velocity on the vapor film thickness is similar qualitatively to what was discussed above in connection with the effect of subcooling. This discussion will not be repeated here for brevity. Of interest, however, is the effect of Da on the vapor film thickness shown in Fig. 5. The dependence of δ_* on angular position becomes weak as Da decreases. For example, for $Da = 10^{-7}$ and for both the sphere and the cylinder, δ_* is practically independent of θ for $\theta < 90$ deg. The impact of Da in going from 10^{-6} to 10^{-4} is much more dramatic than the impact of Da in going from 10^{-4} to 10^{-2}. Much like in Figs. 3 and 4, respectively pertaining to the effect of subcooling and liquid velocity, for a certain value of θ the vapor film thickness for the sphere overtakes that for the cylinder. Figures 3–5 imply that this value of θ remains practically unaffected by changes in one of the system parameters as long as the other two are held fixed.

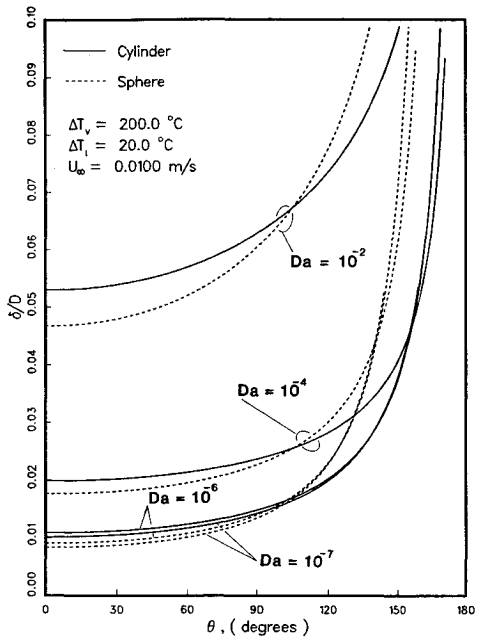

Fig. 5 The effect of the Darcy number on the vapor film thickness: $\Delta T_l = 20°C$, $U_\infty = 0.01$ m/s ($A = 1.32 \times 10^{-2}$, $B = 4.00 \times 10^{-2}$, $M = 1.8 \times 10^{-2}$, $N = 4.60 \times 10^{-2}$).

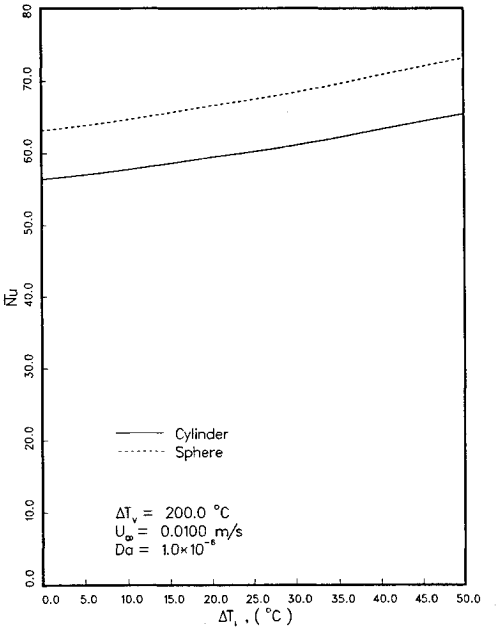

Fig. 7 The effect of subcooling on the overall Nusselt number: $Da = 10^{-6}$, $U_\infty = 0.01$ m/s ($A = 1.32 \times 10^{-2}$).

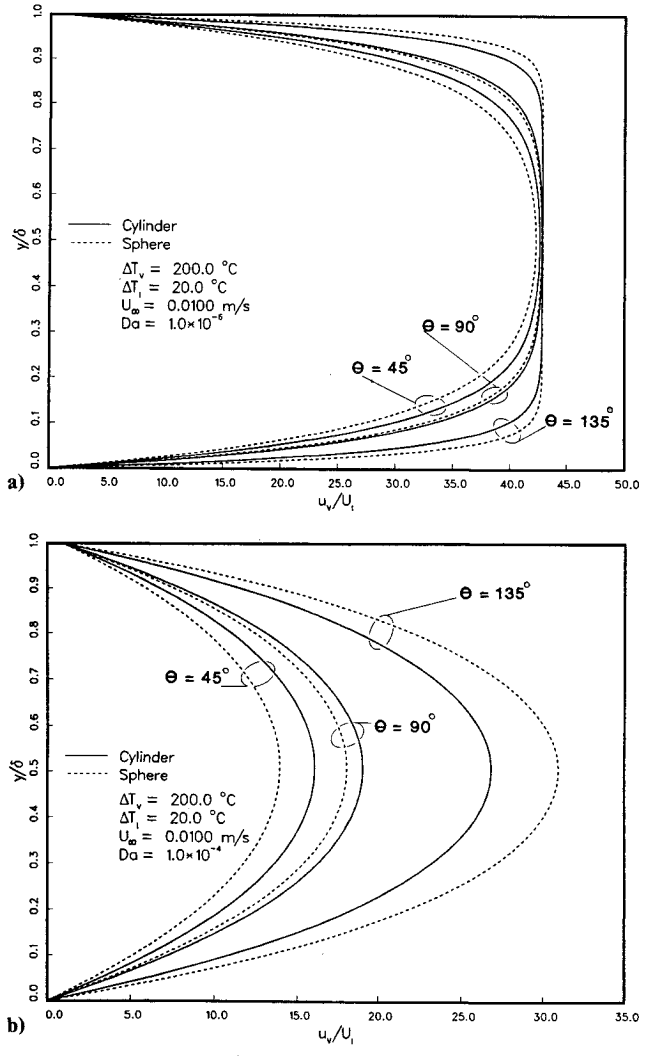

Fig. 6 Velocity profiles in the vapor film: a) $Da = 10^{-4}$, and b) $Da = 10^{-6}$, $\Delta T_l = 20°C$, $U_\infty = 0.01$ m/s ($A = 1.32 \times 10^{-2}$, $B = 4.00 \times 10^{-2}$, $M = 1.80 \times 10^{-2}$, $N = 4.60 \times 10^{-2}$).

Figure 6 shows velocity profiles at various locations around the periphery of the body (cylinder or sphere). As discussed in the previous section, no flow reversal was observed. This property of the flowfield is different from what was found in Ref. 9 for classical fluids where flow reversal occurred for a critical value of the angular coordinate. For flow film boiling in porous media, according to the present results, the flow actually accelerates as θ increases. It appears that the growth of the vapor film thickness with θ is not rapid enough to counteract the vapor accumulation. As a result, the flow of vapor is accelerated to satisfy continuity. The opposite effect has been observed in classical fluids where the vapor flow actually slows down as the angular coordinate increases. The fact that the growth of δ_* with θ is not sufficiently fast is supported by Figs. 3–5, which show that for values of $\theta < 60$ deg (approximately), δ_* is practically independent of θ. Comparing Figs. 6a and 6b we see that decreasing Da (permeability) yields a much flatter vapor velocity profile. From a physical standpoint, the flowfield in Fig. 6a indicates the dominance of the Darcy term in the momentum equation (1). The changing of the profile to parabolic in Fig. 6b illustrates the sizeable contribution of the macroscopic shear effect represented by the second term in the right side of Eq. (1).

Figures 7–9 illustrate, respectively, the effect of the subcooling, liquid velocity, and Darcy number on the overall Nusselt number. In all cases, for the values of parameters examined in this study, the results for the cylinder and sphere exhibit the same qualitative behavior. The values of $\overline{Nu}$ for the sphere are consistently higher than the values of $\overline{Nu}$ for the cylinder. Increasing the subcooling results in higher heat fluxes and, therefore, increases $\overline{Nu}$ (Fig. 7). The deviation between the sphere and the cylinder results becomes more evident as ΔT_B increases. The same is true for the effect of the liquid velocity on $\overline{Nu}$ shown in Fig. 8. The deviation between the cylinder and the sphere results in changes from almost negligible for small values of U_∞ to substantial for large values of U_∞. As expected, $\overline{Nu}$ increases monotonically with U. After an initial sharp rate of increase of $\overline{Nu}$, its dependence on U_∞ becomes practically linear.

Figure 9 indicates a drastic decrease in $\overline{Nu}$ as Da increases for $Da > 10^{-6}$. For small values of Da, a plateau is reached corresponding to the case in which the Brinkman effect is negligible. Decreasing Da alters the shape of the velocity profile (Fig. 6) and yields sharper velocity gradients at the body sur-

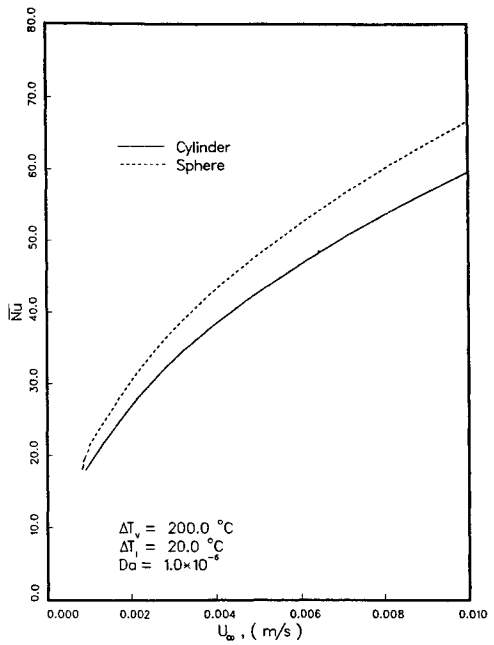

Fig. 8 The effect of liquid velocity on the overall Nusselt number: $Da = 10^{-6}$, $\Delta T_l = 20°C$.

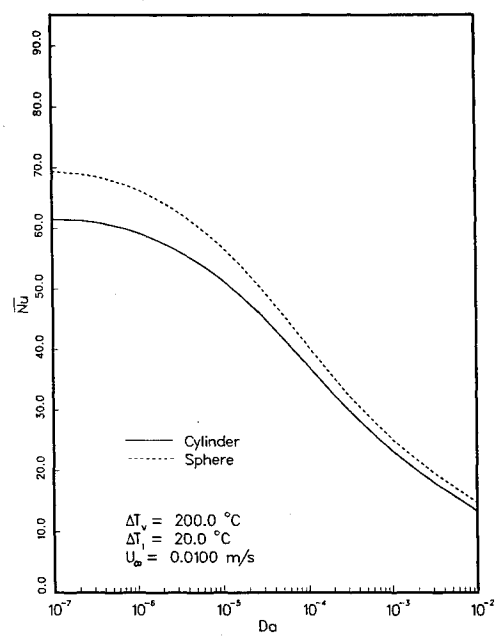

Fig. 9 The effect of Da on the overall Nusselt number: $U_\infty = 0.01$ m/s, $\Delta T_l = 20°C$ ($A = 1.32 \times 10^{-2}$, $B = 4.00 \times 10^{-2}$, $M = 1.80 \times 10^{-2}$, $N = 4.60 \times 10^{-2}$).

face and, hence, enhanced heat transfer. In summary, the presence of the porous matrix augments the heat-transfer process from the body surface to the fluid. A dense porous matrix (small values of Da) may serve as a valuable tool for heat-transfer enhancement.

Conclusions

In this study, we presented an approximate theoretical model for flow film boiling from a horizontal cylinder and from a sphere embedded in porous medium. It was found that the vapor film thickness increases as the angular coordinate θ increases in the region $0 < \theta < \pi$. In the analysis of flow film boiling from submerged bodies, it is commonly assumed that the liquid pressure, governed by Bernoulli's equation, is "impressed" on the vapor layer. This condition creates an adverse pressure gradient for $\theta > 90$, which leads to flow separation or backflow in the vapor film. However, in the case of bodies embedded in porous media, the "impressed" pressure gradient in the vapor film is dictated by Darcy's equation and, consequently, a favorable pressure gradient exists along the circumference of the heater. Therefore, no vapor flow separation takes place. Increasing the subcooling and the liquid velocity and decreasing the Darcy number yields thinner vapor layers.

The heat transfer from the body is enhanced with increasing the subcooling and the liquid velocity, as the results for the overall Nusselt number indicates. The sphere yields higher overall Nusselt numbers than the cylinder of the same diameter. This fact becomes more apparent as the liquid velocity and the subcooling increase. The presence of a dense porous matrix augments the heat-transfer process. Witness to this fact is the drastic increase of $\overline{Nu}$ as Da decreases.

In summary, the simple model outlined in this study yielded a number of interesting results documenting the phenomenon of flow film boiling from a spherical or cylindrical body in porous medium. Future experiments aiming to verify the present theoretical findings are deemed to be appropriate.

Acknowledgment

The authors appreciate the support of Amoco Research and the National Science Foundation during this study.

References

[1]Cheng, P., "Film Condensation Along an Inclined Surface in Porous Medium," *International Journal of Heat and Mass Transfer*, Vol. 24, 1981, pp. 983-990.

[2]Cheng, P. and Verma, A. K., "The Effect of Subcooled Liquid on Film Boiling Above a Vertical Heated Surface in a Porous Medium," *International Journal of Heat and Mass Transfer*, Vol. 24, 1981, pp. 1151-1160.

[3]Ip, P. S.-S. and Minkowycz, W. J., "The Effect of Axial Pressure Variations on Film Boiling About a Heated Vertical Pipe Embedded in a Porous Medium," *Numerical Heat Transfer* (to be published).

[4]Chuah, Y. K. and Carey, V. S., "Boiling Heat Transfer in a Shallow Fluidized Particulate Bed," *Heat Transfer in Porous Medium and Particulate Flows*, edited by L. S. Yao et al., HTD-Vol. 46, 1985, pp. 119-126.

[5]Tsung, V. X., Dhir, V. K., and Singh, S., "Experimental Study of Boiling Heat Transfer from a Sphere Embedded in Liquid Saturated Porous Media," *Heat Transfer in Porous Media and Particulate Flows*, edited by L. S. Yao et al., HTD-Vol. 46, 1985, pp. 127-134.

[6]Tong, T. W. and Subramanian, E., "A Boundary Layer Analysis for Natural Convection in Vertical Porous Enclosures—Use of Brinkman-Extended Darcy Model," *International Journal of Heat and Mass Transfer*, Vol. 28, 1985, pp. 563-571.

[7]Hsu, T. C. and Cheng, P., "The Brinkman Model for Natural Convection About a Semi-Infinite Vertical Flat Plate in Porous Medium," *International Journal of Heat and Mass Transfer*, Vol. 28, 1985, pp. 683-697.

[8]Somerton, C. W. and Catton, I., "On the Thermal Instability of Superposed Porous and Fluid Layers," *Journal of Heat Transfer*, Vol. 104, 1982, pp. 160-165.

[9]Witte, L. C. and Orozco, J., "The Effect of Vapor Velocity Profile Shape on Flow Film Boiling from Submerged Bodies," *Journal of Heat Transfer*, Vol. 106, 1984, pp. 191-197.

[10]Greencorn, R. A., "Flow Phenomena in Porous Media," Dekker, 1983, pp. 65-77.

[11]Kobayasi, K., "Film Boiling Heat Transfer Around a Sphere in Forced Convection," *Journal of Nuclear Science and Technology*, Vol. 2, 1965, pp. 62-67.

[12]Epstein, M. and Hauser, G., "Subcooled Forced Convection Film Boiling in the Forward Stagnation Region of a Sphere or Cylinder," *International Journal of Heat and Mass Transfer*, Vol. 23, 1980, pp. 179-189.

[13]Sideman, S., "The Equivalence of the Penetration Theory and Potential Flow Theories," I. and E. C., Vol. 58, 1966, pp. 54-68.

[14]Ferziger, J. H., "Numerical Methods for Engineering Application," Wiley, New York, 1981, pp. 76-84.